ECN

Energy research Centre of the Netherlands

Wind farm design - When other wind farms are close

A.J. Brand

This report has been presented at the European Offshore Wind 2009 Conference, Stockholm, 14-16 September, 2009

ECN-M--09-127 SEPTEMBER 2009

Wind farm design - When other wind farms are close

A J Brand
ECN Wind Energy, P.O. Box 1, NL 1755 ZG Petten, Netherlands
E: brand@ecn.nl, T: +31 224 56 4775, F: +31 224 56 8214

Abstract This work presents an approach to evaluate the wind climate in a location close to another wind farm. It is shown that the effect of the upstream wind farm can be expressed in various impact parameters, and that these can be determined by using a dedicated planetary boundary layer solver. Apart from the force on the flow due to the wind farm, this solver takes into account the convective as well as the Coriolis forces. The impact parameters include the velocity recovery distance, which is shown to be of the order of a hundred kilometer for the current size of wind farms, and the minimum safe distance, which is shown to be of the order of ten kilometer.

Key words Planetary boundary layer, Offshore wind energy, Wind farm wake, Wind farm interaction

1. Introduction

Over the years offshore wind farms tend to be placed closer together, as already illustrated by the Offshore Windfarm Egmond aan Zee and the Princess Amalia Windfarm in the Netherlands, or Horns Rev I and Horns Rev II in Denmark. Since the separation distance is between 5 and 10 times the wind farm's horizontal length scale, the velocity deficit may be considerable [1][2]. If so, energy production losses and mechanical load increases are expected to be significant. From the developer's point of view the challenge is to determine how large these will be if an otherwise promising site is surrounded by wind farms. To address this design challenge a dedicated planetary boundary layer solver has been developed which allows one to determine the velocity deficit due to an upstream wind farm [3].

In this paper we introduce the concepts relevant to wind farm design and the methodology of this planetary boundary layer solver. We show how various impact parameters are determined including the velocity recovery distance (where the velocity reaches a given percentage of the upstream value) and the minimum safe distance (beyond which the velocity deficit is less than 0.5 m/s if the upstream wind speed is equal to the cut-in wind speed).

The outline of the paper is as follows. First, in section 2 previous work on wind farm wakes is presented. Next, section 3 introduces concepts in the form of wind farm design parameters, meteorological design parameters and impact parameters. Section 4 describes the planetary boundary layer flow solver. Section 5 addresses results obtained with the solver: validations (results that can be compared to measured data) and predictions (results that can be used for future wind farms). Finally, the conclusions are presented in section 6.

2. Previous work

A wind farm wake study requires simulation of mesoscale atmospheric flow together with energy extraction/redistribution due to wind turbines. In this section first we present an overview of studies that were published by the year 2007. Next we identify the various approaches in these studies and we finish with a critical review of these approaches.

Liu et al. developed a numerical model based on the primitive equations in order to study the behaviour of turbulent wakes behind large-scale wind turbines [4]. This model is based on a numerical solution of the Navier-Stokes equations for the planetary boundary layer with the hydrostatic approximation, in combination with a Monin-Obukhov description of the turbulent diffusivities. To demonstrate the utility of the model, it was applied to three different configurations of wind turbine arrays, among which one wind turbine immediately downwind of another. The results of the model simulations were found not only to retrieve major features of turbulent wakes

observed behind wind turbines but also to compare favourably with corresponding measurements from wind tunnel experiments.

Hegberg and Eecen analytically modeled the effect of a wind farm on the atmospheric boundary layer [5]. First they estimate the artificial roughness length of the wind farm, and next they calculate the internal boundary layer which results from the roughness change due to the wind farm. With this information the new turbulent drag force and subsequently the new equilibrium between the forces (turbulent drag force, the Coriolis force and the pressure gradient force) are determined. From that equilibrium the new wind speed and direction are calculated, which are found to be quite different from the conditions outside the wind farm.

Frandsen et al. developed an analytical model for the flow in and near a wind farm [6]. The model distinguishes between two flow directions (parallel to the rows in a rectangular wind turbine configuration, and not parallel) and identifies three flow regimes (multiple wakes, merging wakes from neighbouring rows, and equilibrium between the wind farm and the boundary layer). The multiple wakes model and the merging wakes model were derived from the Lanchester-Betz theory, whereas the equilibrium model was derived from the geostrophic drag law. The effect of turbulence is included in the modeling of the equilibrium regime only by using the skin friction velocity and the surface roughness length. The model is reported to predict offshore wind recovery distances in the range between 2 and 14 km.

Hegberg et al. developed a numerical model in order to study the effect of a wind farm on the planetary boundary layer [7]. Similar to their preceding model [5], a wind farm is modeled as surface roughness but now a number of sub-models are proposed to do so. In addition they add an innovative element in the form of an atmospheric boundary layer model which, apart from velocity, also takes temperature into account. Turbulence is modeled in terms of Reynolds stresses of velocity and temperature, which gives the possibility to treat small departures from the neutral situation.

Baidya Roy et al. applied the Regional Atmospheric Modeling System to explore the possible impacts of a large (100x100 km^2) onshore wind farm in the Great Plains [8]. This model solves the full three-dimensional compressible nonhydrostatic dynamic equations, a thermodynamic equation and a set of microphysics equations. The system of equations is closed with a Mellor-Yamada scheme that explicitly solves for turbulent kinetic energy while other second-order moments are parameterized. A wind turbine was approximated as a sink of energy (operating at a fixed power coefficient of 0.4) and source of turbulence (adding a fixed amount of turbulent kinetic energy), and the wind farm was created by assuming an array of such turbines. Results show that the wind farm significantly slows down the wind at the turbine hub-height level.

Rooijmans simulated the meteorological effects of a large-scale (150x60 km^2) offshore wind farm in the North Sea by using the MM5 mesoscale model [9]. The wind farm was simulated by introducing a higher roughness length (0.5 m) in the area of the wind farm. The meteorological effects were examined by comparing model runs with and without wind farm. Turbulent kinetic energy, cloud formation, precipitation and wind speed reduction were studied. As to wind reduction the MM5 model was found to yield comparable results (in and near the wind farm wind speed reduction up to 50% in a high wind speed case) as obtained from a conceptual model which calculates the reduction of horizontal wind speed from a balance between loss of horizontal momentum and replenishment from above by turbulent fluxes.

These studies can be subdivided into two categories: self-similar approaches and mesoscale approaches. In a self-similar approach the convective force and the spanwise turbulent flux gradients are assumed to dominate the flow, allowing for standard wake-like solutions [6][7]. In a mesoscale approach, on the other hand, the flow is assumed to be dominated by the Coriolis force and the vertical turbulent flux gradients, opening the door to either extra surface drag approaches [5] or more generic mesoscale approaches [4][8][9].

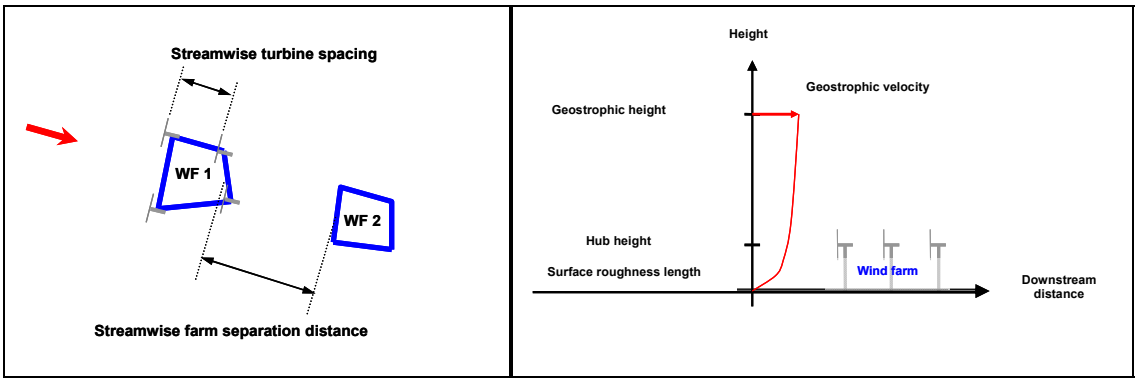

Figure 1: Top view (left) and side view (right) of the wind farm design parameters

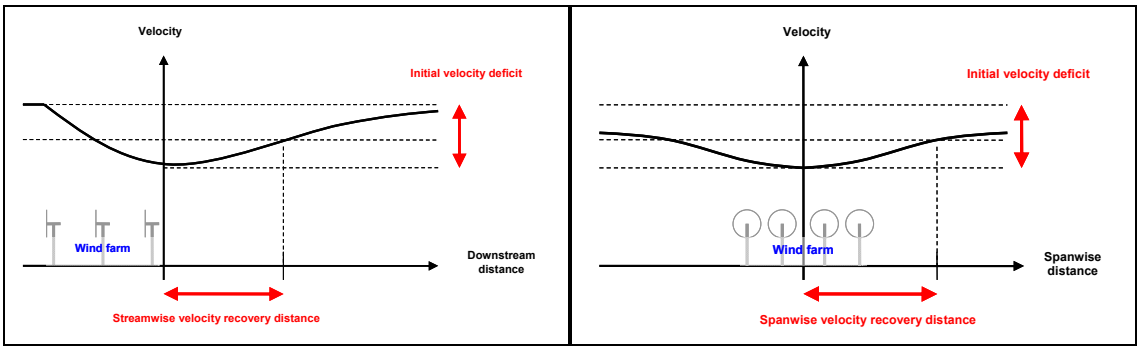

Figure 2: Impact of a wind farm on the velocity in streamwise direction (left) and spanwise direction (right)

In section 4 of this report we will show that neither the self-similar wake approach nor the extra surface drag approach is sufficient because over the separation distance between wind farms the convective and the Coriolis forces are of equal order of magnitude. Since this implies that a wind farm wake may be deflected, these terms are retained in the model which is presented in section 4. Although this balance of forces was already implicitly recognized in the more generic approaches, these studies lack realistic formulations for the turbulence and the wind turbines.

3. Design parameters and impact parameters

Parameters that are used when designing a wind farm include wind farm design parameters and meteorological design parameters.

The wind farm design parameters have been set such that the production of a wind farm is optimal (figure 1). These include hub height, rotor diameter and nominal power of the wind turbines, as well as distance between the turbines and distance to other wind farms. The meteorological design parameters on the other hand are given constraints which characterize the wind climate at a site. These include the geostrophic velocity (that is a wind speed which is independent of what happens close to the surface), the height where that velocity is reached, and the surface roughness length (that is the length scale which characterizes the roughness of the surface).

Impact parameters, as their name suggests, measure the impact of a wind farm on the velocity (figure 2). Impact parameters include velocity deficit, velocity recovery distance, minimum safe distance, and disturbed sectors in the wind rose. Velocity deficit is the difference between the upstream velocity and the downstream velocity. In general the velocity deficit decays from an initial value to a much lower value. The distance where the velocity reaches a given fraction, for example 99%, of the upstream value is the velocity recovery distance. The minimum safe distance is a similar measure, indicating the distance beyond which the velocity deficit is less than 0.5 m/s. Since these distances depend on the upstream wind direction, a second wind farm ex-

periences wind direction sectors where the velocity deficit is significant, or, in other words, a disturbed wind rose.

4. Method

4.1 Overview

In order to determine the impact of an upstream wind farm on the wind at a given downstream site, a dedicated flow solver has been developed. The two principles behind this solver (a physical and a numerical) are described in the sections 4.2 and 4.3. The actual impact parameters warrant a translation from the calculated grid-cell averaged values into the required single point values. The model which is used for this purpose is described in section 4.4.

4.2 Physical principle

According to the physical principle neutral planetary boundary layer flow with wind farms is steady and two-dimensional, where the forces all have the same order of magnitude. The physical principle follows from an analysis which includes (figure 3):

(a) The definition of the flow problem,
(b) The decomposition of the wind speed and the way it depends on the height above the surface and the pressure gradients, and
(c) An analysis of the relevant length and velocity scales.

It ultimately leads to the set of governing equations:

$$\bar{u}\frac{\partial \bar{u}}{\partial x} + \bar{v}\frac{\partial \bar{u}}{\partial y} = +f_\phi\left(\bar{v} - v_g\right) - \frac{\partial \overline{u'v'}}{\partial y} - \frac{\partial \overline{u'w'}}{\partial z} + \overline{a_x} \tag{1}$$

$$\bar{u}\frac{\partial \bar{v}}{\partial x} + \bar{v}\frac{\partial \bar{v}}{\partial y} = -f_\phi\left(\bar{u} - u_g\right) - \frac{\partial \overline{v'v'}}{\partial y} - \frac{\partial \overline{v'w'}}{\partial z} + \overline{a_y} \tag{2}$$

convective force	Coriolis force	spanwise turb. flux gradient	vertical turb. flux gradient	external force

$$\frac{\partial \bar{u}}{\partial x} + \frac{\partial \bar{v}}{\partial y} = 0\,, \tag{3}$$

where $\bar{u}$ and $\bar{v}$ indicate the Reynolds averaged streamwise and spanwise component of the velocity, $\overline{u'v'}$ etc indicate the turbulent momentum fluxes, and a indicates the deceleration of the flow due to a wind farm.

In contrast to standard geostrophic flow, modeled by the momentum equations

$$0 = +f_\phi\left(\bar{v} - v_g\right) - \frac{\partial \overline{u'w'}}{\partial z} + \overline{a_x}$$

$$0 = -f_\phi\left(\bar{u} - u_g\right) - \frac{\partial \overline{v'w'}}{\partial z} + \overline{a_y}\,,$$

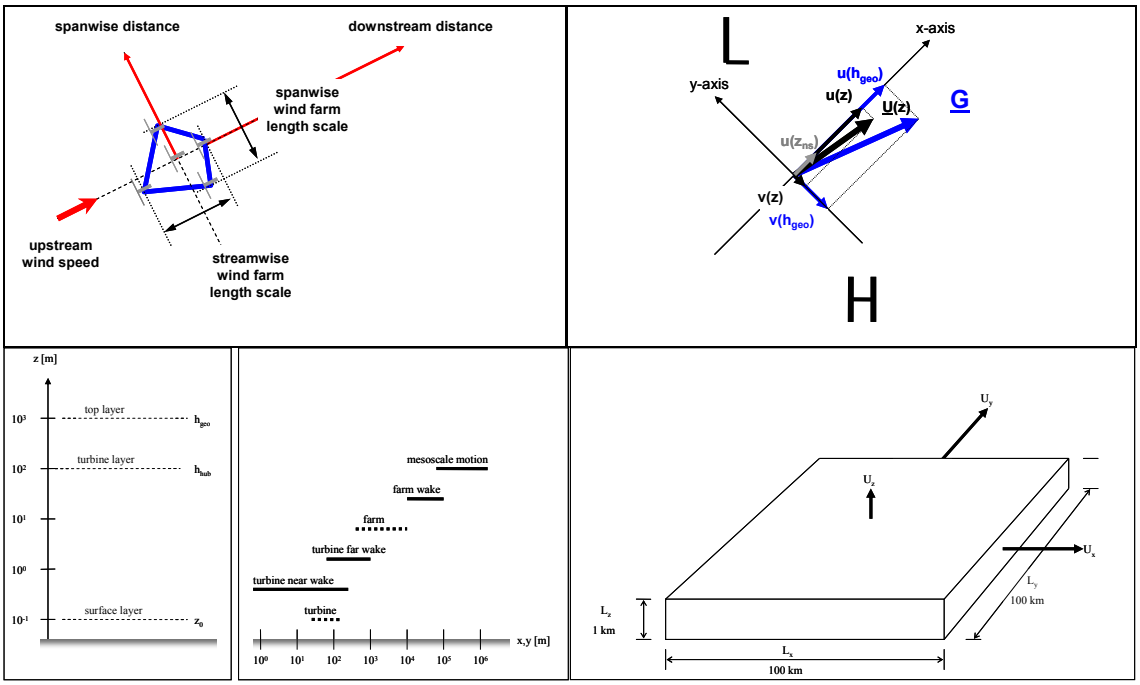

Figure 3: Sketch of the physical principle: definition of the flow problem (top left), velocity decomposition (top right), two-dimensional length and velocity scales (bottom right) and vertical and horizontal length scales (bottom left)

in equations 1 and 2 the convective force and the y-wise turbulent momentum flux gradients are significant, which rules out the extra surface drag approaches which are usually applied to solve these momentum equations. In addition, in contrast to general wake flow, modeled by the momentum equations

$$-\bar{u}\frac{\partial \bar{u}}{\partial x} + -\bar{v}\frac{\partial \bar{u}}{\partial y} = -\frac{\partial \overline{u'v'}}{\partial y} + \bar{a}_x$$

$$-\bar{u}\frac{\partial \bar{v}}{\partial x} + -\bar{v}\frac{\partial \bar{v}}{\partial y} = -\frac{\partial \overline{v'v'}}{\partial y} + \bar{a}_y ,$$

in equations 1 and 2 the Coriolis force and the vertical turbulent momentum flux gradients are significant, ruling out self-similar wake approaches.

4.3 Numerical principle

According to the numerical principle the numerical representation of the momentum equations allows for:

(a) An implicit solution of the two horizontal velocity components in vertical direction, iterating on the turbulent viscosity while employing a mass-energy conserving scheme, and
(b) A marching solution in the horizontal directions.

To this end backward differences have been chosen. In addition the continuity equation 3 is satisfied by employing the Lagrange multiplier method to the velocity components that satisfy the momentum equation. Because of the mixed implicit/explicit character the solver is computationally fast and cheap.

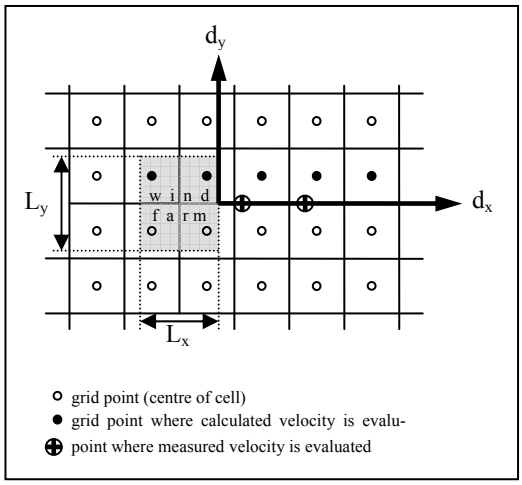

Figure 4: Horizontal lay-out of the grid cells in relation to the horizontal area covered by a wind farm, and definition sketch of downstream distance d_x, spanwise distance d_y, streamwise wind farm length scale L_x and spanwise wind farm length scale L_y. Also indicated are the points where measured velocity is evaluated in the validation study

4.4 Point velocity model

The solver allows one to calculate the velocity near a wind farm. It is important to note that a resolved velocity is the average value of the velocities in the grid cell, which is in contrast to the general interpretation in the form of a single point value. To be more specific the solver allows one to calculate the grid-cell averaged values of the velocity deficit downstream a wind farm, which values subsequently are translated into single-point values by using a point velocity wake model. Inspired by the literature [10][11][12], this model has power law decay in streamwise direction d_x and Gaussian decay in spanwise direction d_y:

$$U(d_x, d_y) = U_0 - \Delta U(d_x, d_y) \text{ with } \frac{\Delta U(d_x, d_y)}{\Delta U_{ini}} = \left(\frac{d_x}{d}\right)^m \exp\left\{-\frac{d_y^2}{(b_1 d_x + b_0)^2}\right\}.$$

(See figure 4 for the definition of d_x and d_y.) Here m is the exponent of the streamwise velocity deficit decay, ΔU_{ini} is the initial velocity deficit, d = 2D is the streamwise scale of the velocity deficit decay, b_1 is the decay rate of the wake width, and b_0 is the initial wake width. In the actual translation the grid-cell averaged values are fit to the point velocity wake law, from which fit the exponent m and the initial velocity deficit ΔU_{ini} are determined.

5. Results

5.1 Overview

For a relatively small number of calculations the outcome can be compared to measured data. (Unfortunately, the measured data can not be shown because of confidentiality reasons.) This is what we refer to as validations, in contrast to predictions which are the outcome of calculations where measured data is not yet available.

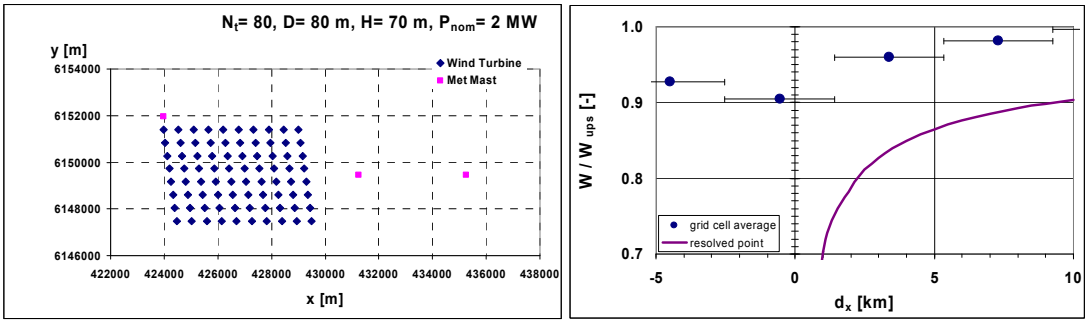

Figure 5: Layout of the Horns Rev wind farm (left) and velocity W relative to the upstream velocity W_{ups} of 6 m/s as a function of distance d_x downstream (right)

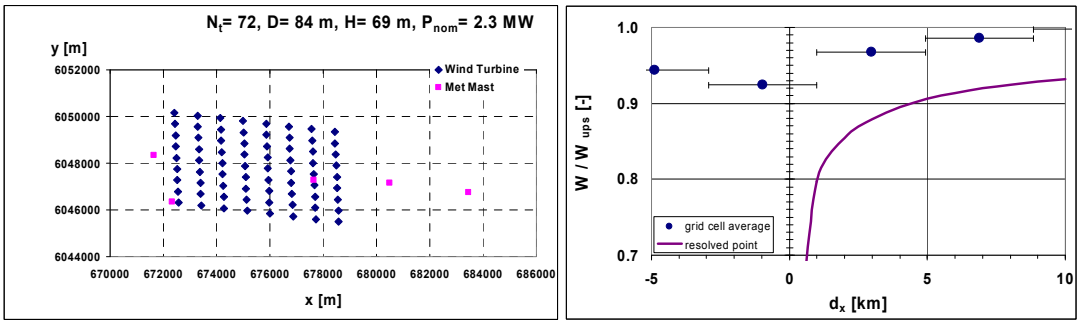

Figure 6: Layout of the Nysted wind farm (left) and velocity W relative to the upstream velocity W_{ups} of 6 m/s as a function of distance d_x downstream (right)

5.2 Validation

Validation data from the Horns Rev wind farm comprise confidential single-point wind speed measured at three meteo masts. For the cases where the flow direction is parallel to the turbine rows, one meteo mast provides the upstream velocity whereas the other two masts provide downstream velocities. The four dots in figure 5 show the grid-cell averaged velocity relative to the upstream velocity in and behind the wind farm. Also shown are horizontal lines which indicate the streamwise size of the grid cells. The solid line, on the other hand, shows the single point velocity as a function of distance behind the farm, as obtained by fitting the grid-cell averaged values to the velocity deficit decay law. It is found that the relative velocity deficit is of the order of 17% at 2 km, and 10% at 6 km. Also a reasonable agreement is found between the measured values and those from the wake deficit decay model.

Validation data from the Nysted wind farm also comprises data from three meteo masts, but the layout of the wind farm and the positions of the meteo masts are different. Again we consider flow cases where the flow direction is parallel to the turbine rows. The figure 6 with the grid-cell averaged velocities and the single point velocities reveals much the same information as the preceding ones: a relative velocity deficit of about 15% at a downstream distance of 2 km, and 10% at 5 km.

Information on the velocity recovery distance and the minimum save distance are compiled in table 1.

Table 1: Velocity recovery distance and minimum save distance as a function of wind speed

Wind speed [m/s]	Velocity recovery distance [km]	Minimum save distance [km]
6	178	6.1
8	554 - 1047	6.5 – 24.4
10	90 - 832	5.1 – 33.9

The velocity recovery distance, which is the downstream distance where the velocity has recovered to 99% of the upstream value, is found to be several hundreds of kilometer. And the minimum save distance, which is the distance beyond which the velocity deficit is less than 0.5 m/s, is found to be of the order of 10 km.

5.3 Prediction

We will consider a hypothetical wind farm having a baseline nominal power density of 5 MW/km^2, and will look at the impact of changes in this baseline nominal power density on the initial velocity deficit, the velocity recovery distance and the minimum save distance (figure 7).

First we consider the impact on the initial velocity deficit in the wake of the wind farm. At 5 MW/km^2 the initial velocity deficit is 40% of the upstream velocity. Decreasing the power density, for example by increasing the distance between the turbines, results in a lower value of the initial velocity deficit. In addition it shows that an increase of the power density, for example by putting the turbines closer together, results in a higher initial velocity deficit.

Next we study the impact of the nominal power density on the velocity recovery distance. At 5 MW/km^2 the velocity recovery distance is of the order of 10 km. A reduction of the power density results in a smaller value but it still is of the same order of magnitude. An increase, on the other hand, gives values which are an order of magnitude higher.

The same picture emerges for the minimum save distance which is about 1 km if the nominal power density is 5 MW/km^2, but which is considerably larger if the nominal power density is larger.

6. Conclusions

In this paper it has been shown that the local wind climate downstream of other wind farms can be determined by applying a flow model of planetary boundary layer flow which includes wind farms, and which takes the Coriolis as well as the convective forces into account. Furthermore various impact parameters have been introduced which can be determined by applying the flow solver. These impact parameters include the velocity recovery distance, which is of the order of several hundreds of kilometer, and the minimum save distance, which is of the order of ten kilometer.

Acknowledgements

This work was performed in the framework of the Dutch Ministry of Economic Affairs BSIK programme We@Sea, project "Windenergiecentrale Noordzee - Parkinteractie" (We@Sea/BSIK 2005/002).
Measured data by courtesy of L.E. Jensen of Dong Energy A/S as prepared by K.S. Hansen in the framework of the European UPWIND research project under contract with the European Commission (CE Contract Number 019945 (SES6)).

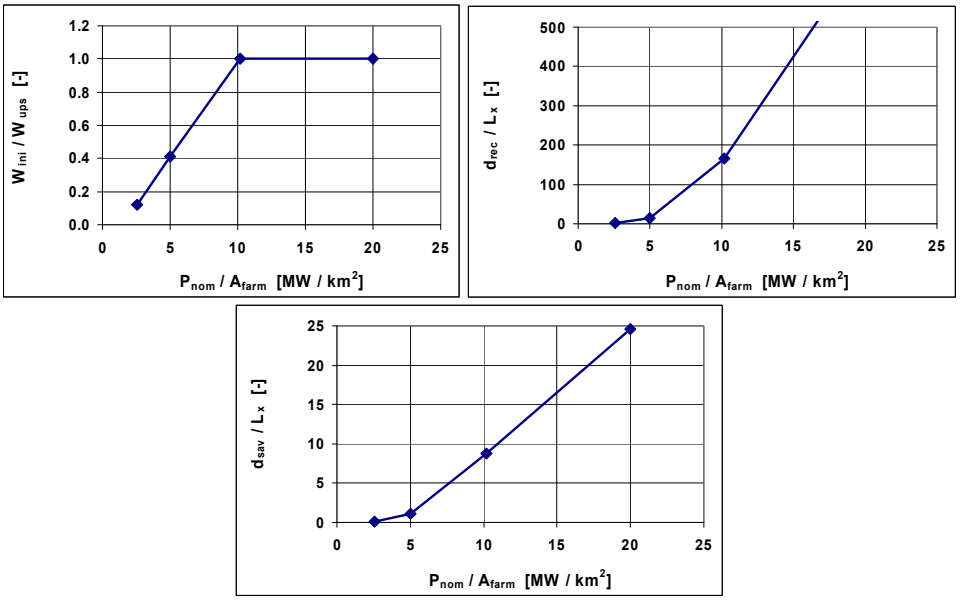

Figure 7: Initial velocity deficit (top left), velocity recovery distance (top right) and minimum save distance (bottom) for a hypothetical wind farm as a function of nominal power density

References

1. Christiansen MB and Hasager CB, Wake studies around a large offshore wind farm using satellite and airborne SAR, In: 31st Int. Symp on Remote Sensing of Environment, St Petersburg, Russian Federation, 2005
2. Barthelmie R et al., Flow and wakes in large wind farms in complex terrain and offshore, European Wind Energy Conference 2008, Brussels, Belgium, 2008
3. Brand AJ, Wind power plant North Sea - Wind farm interaction, ECN Wind Energy, Report ECN-E--09-041, 2009
4. Liu M-K et al., Mathematical model for the analysis of wind-turbine wakes, J. Energy, Vol. 7, No. 1, pp. 73-78, 1983
5. Hegberg T and Eecen PJ, The effect of large wind farms on the atmospheric boundary layer, In: Proc. Global Wind Power Conference 2002, Paris, France, 2002
6. Frandsen S et al., The necessary distance between large wind farms offshore - Study, Risø National Laboratory, Report Risø-R-1518(EN), 2004
7. Hegberg T et al., Turbine interaction in large offshore wind farms - Atmospheric boundary layer above a wind farm, Report ECN-C--04-033, 2004
8. Baidya Roy S et al., Can large wind farms affect local meteorology? J. Geoph. Research, Vol. 109, D19101, 2004
9. Rooijmans P, Impact of a large-scale offshore wind farm on meteorology - Numerical simulations with a mesoscale circulation model, Universiteit Utrecht, Masters thesis, 2004
10. Milborrow DJ, The performance of arrays of wind turbines, J. Industrial Aerodynamics, 5 (1980), pp. 403-430, 1980
11. Elliott DL, Status of wake and array loss research, In: Proc. Windpower91, Palm Springs, California, 1991
12. Barthelmie R et al., Efficient Development of Offshore Windfarms (ENDOW), Report Risø-R-1407(EN), 2003